Controlling edge states of zigzag carbon nanotubes by the Aharonov-Bohm flux

K. Sasaki,[1,*] S. Murakami,[2] R. Saito,[3] and Y. Kawazoe[1]
[1]*Institute for Materials Research, Tohoku University, Sendai 980-8577, Japan*
[2]*Department of Applied Physics, University of Tokyo, Hongo, Bunkyo-ku, Tokyo 113-8656, Japan*
[3]*Department of Physics, Tohoku University and CREST, JST, Sendai 980-8578, Japan*
(Received 19 January 2005; published 3 May 2005)

It has been known theoretically that localized states exist around the zigzag edges of a graphite ribbon and of a carbon nanotube, whose energy eigenvalues are located between conduction and valence bands. We find that in metallic, zigzag single-walled, carbon nanotubes two of the localized states become critical, and that their localization length is sensitive to the mean curvature of a tube, and it can be controlled by the Aharonov-Bohm flux. The curvature-induced mini gap closes by the relatively weak magnetic field. A conductance measurement in the presence of the Aharonov-Bohm flux can give information about the curvature effect and the critical states.

DOI: 10.1103/PhysRevB.71.195401 PACS number(s): 73.63.Fg, 72.15.−v, 72.80.Rj

Prior theoretical studies on zigzag carbon nanotubes clarified that they can exhibit either a metallic or semiconducting energy band, depending on their chiral vectors.[1] It has been shown theoretically[2] and experimentally[3] that even in "metallic," zigzag single-walled carbon nanotubes (SWCNTs) a finite curvature opens small energy gaps. Therefore, all zigzag SWCNTs have finite energy gaps.

On the other hand, Fujita *et al.*[4] theoretically showed that localized states (edge states) emerge at graphite zigzag edges. The edge states are plane-wave modes along the edges and their energy eigenvalues are between the valence band and the conduction band (zero-energy states). Since a graphite sheet with zigzag edges can be rolled to form a zigzag SWCNT, the edge states are supposed to be localized at both edges of the zigzag SWCNT and are predicted to make a certain magnetic ordering, depending on the nanotube length and radius.[5] In this case, a zigzag nanotube has not only bulk (extended) states with a finite energy gap, but also zero-energy, localized edge states. Although several properties of the edge state have been investigated,[6] the physical relationship between the electrical properties of bulk states and edge states remains to be clarified.

In this paper, to investigate this relationship, we study an effect of the Aharonov-Bohm (AB) flux along the metallic, zigzag nanotube axis. Among the Fujita's edge states of metallic, zigzag SWCNTs, we will show that there exist "critical states." Their wave functions, and in particular their localization lengths, are sensitive to the following two perturbations: the curvature and the AB flux. These perturbations are new ingredients for cylindrical geometry and are absent in the flat graphene sheet. Other edge states are hardly affected by these perturbations and their wave functions remain strongly localized at the edge. The main purpose of this paper is to clarify the dependence of the critical states on the AB flux and the relationship between the wave functions at the bulk and at the edge. This dependence can be examined by a conductance measurement in the presence of the AB flux. We note that such an AB flux applied along the SWCNT axis (see Fig. 1) has already been realized in experiments.[7,8]

Because the unit cell is composed of two sublattices, A and B, we write the wave functions as $|\Psi_k\rangle = {}^t[\psi_A(k), \psi_B(k)]$, where k is a discrete wave vector around the tubule axis. By fixing the chiral vector[1] as $C_h=(n,0)$, we obtain $k=2\pi\mu/|C_h|$ ($|C_h|=\sqrt{3}a_{cc}n$) where μ ($=1,\ldots,n$) is an integer and $a_{cc}\approx 1.42$ Å is the carbon-carbon bond length. We analyze the system using the nearest-neighbor tight-binding Hamiltonian, $\mathcal{H}=\Sigma_{a=1,2,3}\Sigma_{i\in A}(V_\pi+\delta V_a)a_{i+a}^\dagger a_i+\text{H.c.}$ "A" (in the summation index) denotes an A sublattice, a_i and $a_i^\dagger$ are canonical annihilation-creation operators of the electron at site i, and site $i+a$ indicates the nearest-neighbor sites ($a=1,2,3$) of site i. We include the curvature effect as the bond-direction-dependent hopping integral, $V_\pi+\delta V_a$. We ignore the electron spin for simplicity.

The energy eigenequation, $\mathcal{H}|\Psi_k\rangle = E|\Psi_k\rangle$, becomes

$$\epsilon\phi_A^{J+1} = \phi_B^J + g\phi_B^{J+1} \quad (J=0,\ldots,N-1), \tag{1}$$

$$\epsilon\phi_B^J = \phi_A^{J+1} + g\phi_A^J \quad (J=0,\ldots,N-1), \tag{2}$$

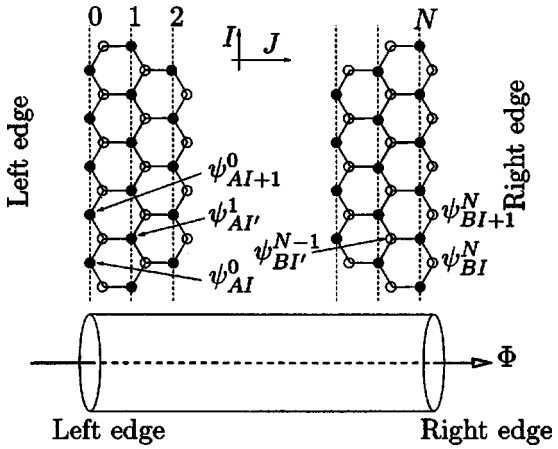

FIG. 1. Lattice structure of a zigzag carbon nanotube. The filled (open) circle indicates the A (B) sublattice. Both the left and right edges are Fujita's edges.

$$\epsilon\phi_A^0 = g\phi_B^0, \quad \epsilon\phi_B^N = g\phi_A^N, \tag{3}$$

where we define

$$\epsilon \equiv \frac{E}{(V_\pi + \delta V_1)}, \quad g \equiv 2\frac{(V_\pi + \delta V_2)}{(V_\pi + \delta V_1)} \cos\frac{\pi(\mu - n_\Phi)}{n}. \tag{4}$$

Here, we write the wave function at site (I,J) of the $A(B)$ sublattice as $\psi^J_{(A,B)I}(k) = \exp(i2\pi I\mu/n)\phi^J_{(A,B)}(\mu)$ (see Fig. 1). We assume $\delta V_2 = \delta V_3$ in the Hamiltonian because of the mirror symmetry along the axis of a zigzag nanotube. The effect of the AB flux is included in g of Eq. (4) by the replacement, $\mu \to \mu - n_\Phi$, where $n_\Phi \equiv \Phi/\Phi_0$ is the number of flux quantum, Φ_0.

By solving Eqs. (1)–(3), we obtain an analytical form of the energy eigenfunction as

$$\phi_A^J = \left[\frac{1}{g}\frac{\sin J\phi}{\sin\phi} + \frac{\sin(J+1)\phi}{\sin\phi}\right]\phi_A^0, \tag{5}$$

$$\phi_B^J = \left[\frac{\sin(J+1)\phi}{\sin\phi}\right]\phi_B^0 \quad (J = 0, \ldots, N), \tag{6}$$

where ϕ satisfies

$$2\cos\phi = \frac{\epsilon^2 - g^2 - 1}{g} \equiv \kappa. \tag{7}$$

The energy eigenvalue is determined by the boundary condition of Eq. (3). Using Eqs. (5) and (6), we get

$$\frac{\sin(N+1)\phi + g\sin(N+2)\phi}{\sin\phi} = 0. \tag{8}$$

This equation corresponds to the vanishing wave function at the fictitious A sites of $J = N+1$, i.e., $\phi_A^{N+1} = 0$. Most of the solutions for ϕ in Eq. (8) are real, as we explain later. Such real solutions represent extended states and satisfy $\kappa^2 \leqslant 4$.

In addition, there can be localized states, where ϕ has an imaginary part and $\kappa^2 > 4$. Their localization lengths are proportional to the inverse of the imaginary part of ϕ. We examine if the boundary condition allows such a localized state. The complex solutions of Eq. (8) can be written as $\phi = i\varphi$ or $\phi = \pi + i\varphi$, where φ is a real number. The former case, $\phi = i\varphi$, corresponds to $\kappa > 2$. In this case, Eq. (8) becomes

$$\sinh(N+1)\varphi + g\sinh(N+2)\varphi = 0. \tag{9}$$

Due to $|\sinh(N+2)\varphi| > |\sinh(N+1)\varphi|$, we obtain $-1 < g < 0$. The latter case, $\phi = \pi + i\varphi$, corresponds to $\kappa < -2$ and $0 < g < 1$. When $|g| \geqslant 1$, on the other hand, Eq. (8) does not allow complex solutions, and therefore there is no localized state in this region. Because the boundary condition implies $g = -e^{+\varphi} + \mathcal{O}(e^{2N\varphi})$ for $\varphi < 0 (-1 < g < 0)$ and $g = e^{-\varphi} + \mathcal{O}(e^{-2N\varphi})$ for $\varphi > 0 (0 < g < 1)$, the energy eigenvalues for the localized states are $\epsilon = \pm\mathcal{O}(e^{-N|\varphi|})$, exponentially small as a function of nanotube length.

By a more elaborate analysis, for a fixed k, we can analytically show that (i) for $|g| \geqslant (N+1)/(N+2)$, all the $2(N+1)$ states are extended, (ii) for $0 < g < (N+1)/(N+2)$, there are $2N$ extended states and two localized states with

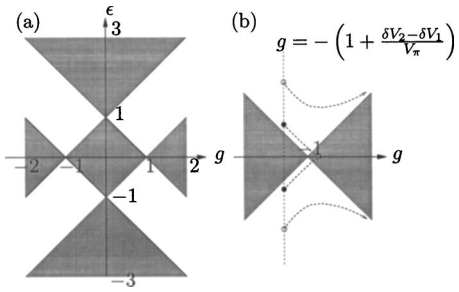

FIG. 2. (a) Region for localized states $\kappa^2 > 4$ shown as the shaded area in the (g,ϵ) plane. Whether localized states are allowed depends on the boundary condition. If the figure is rewritten in terms of k and E, the empty region reproduces the well-known band structure for the graphene sheet. (b) When we ignore the curvature effect, there are states with $g = -1$ in the absence of the AB flux. The curvature effect displaces the states onto the line $g = -[1 + (\delta V_2 - \delta V_1)/V_\pi]$. The AB flux changes the value of g, and the eigenstates will make trajectories like the dashed curves in the figure. The two extended states (filled circles) become localized as they run into the shadow region. The eigenstates, except for these two states, remain extended (open circles).

Re $\phi = \pi$, and (iii) for $-(N+1)/(N+2) < g < 0$, there are $2N$ extended states and two localized states with Re $\phi = 0$. For each wave vector k satisfying $|g| < (N+1)/(N+2)$, the two localized states have energies with opposite signs, $\epsilon = \pm\mathcal{O}(e^{-N|\varphi|})$. Each of the two states is localized near both edges. In the left (right) edge, it is localized in the A (B) sublattice. Henceforth we consider the length N of the nanotube to be large; the localized states are then allowed for $|g| < 1$.

The critical condition, $\kappa^2 = 4$, separates the extended and the localized states. We plot the lines of the critical condition in the (g,ϵ) plane in Fig. 2(a). The shadow regions satisfy $\kappa^2 > 4$, representing localized states. By applying the AB flux, each state moves and makes a trajectory in the (g,ϵ) plane. Suppose one extended state, located outside of the shaded region, comes across the boundaries $\kappa^2 = 4$ between the empty and shaded regions. It means that the extended state turns into a localized state. On the verge of the transition the state becomes "critical," when $g = \pm(N+1)/(N+2) \approx \pm 1$ and $\epsilon = \pm 1/(N+2)$. If we assume $\delta V_a = 0$ and there is no external magnetic field, this condition for g is satisfied only in metallic, zigzag nanotubes, namely, when n is a multiple of 3 and $\mu_1/n = \frac{1}{3}$ or $\frac{2}{3}$ [see Eq. (4)]. When it is satisfied, the states with $g = \pm 1$, $\epsilon \approx 0$ are located very close to the critical line $\kappa^2 = 4$, and thus they can be easily controlled by external perturbations, as we see later.

The cylindrical geometry of nanotubes yields a finite-mean curvature and induces a change of the hopping integral δV_a.[2,9] The scaling of the curvature gives $\delta V_a/V_\pi \approx \mathcal{O}(a_{cc}^2/|C_h|^2)$. The values of g are then driven away from $g = \pm 1$ to

$$g \approx \pm\left(1 + \frac{\delta V_2 - \delta V_1}{V_\pi}\right) + \sqrt{3}\frac{\pi}{n}n_\Phi. \tag{10}$$

From the experimental data of the minigap in metallic, zigzag nanotubes,[3] we estimate[10] $\delta V_2 - \delta V_1 = \pi^2 V_\pi/8n^2$. Thus, in

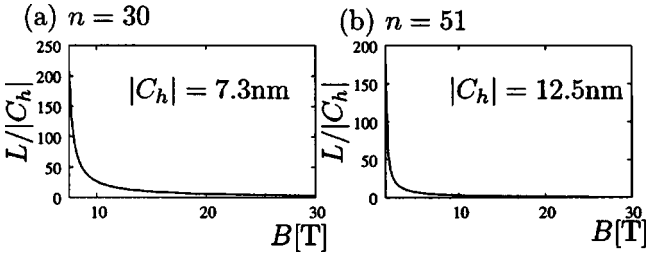

FIG. 3. Localization length of the critical state for (a) $n=30$ and (b) $n=51$ zigzag nanotubes. The horizontal axis is a magnetic field, B T, (a) $7.5 \leqslant B \leqslant 30$ and (b) $1.6 \leqslant B \leqslant 30$.

the absence of the AB flux, these states have $|g|>1$ and are not critical, but extended. However, the AB flux can make one of g within $|g|<1$, which implies that two extended states become localized [see Fig. 2(b)]. At the transition $|g|=1$, there are two critical states with energies very close to zero. In the thermodynamic limit these states have zero energies and infinite localization lengths; therefore, the system becomes gapless at this magnetic-field-induced transition. The values of g for other extended states and zero-energy localized states are far from ± 1; therefore, other extended (localized) states remain extended (localized) even with this external magnetic field.

One of the important questions is whether the AB flux required for such a transition is experimentally accessible or not. We calculate the magnetic field required to close the curvature-induced minigap. From Eq. (10), we find $\bar{n}_\Phi=\pi/(8\sqrt{3}n)$ is necessary to close the minigap for $g=-1$ (for $g=1$, $-\bar{n}_\Phi$ is necessary). This AB flux corresponds to the magnetic field $B \approx 2\times 10^5/n^3$ T. Thus, B is accessible if $n>20$. For a zigzag nanotube with $C_h=(n,0)$, the flux quantum Φ_0 corresponds to the magnetic field $B_n=B_1/n^2$ T ($B_1 \equiv 8.5\times 10^5$ T), and therefore the experimentally accessible magnetic flux corresponds to $|n_\Phi| \ll 1$. For instance, we have $B_9 \approx 10^4$ T, which is well beyond an accessible magnetic field $\approx 10^2$ T, and we can attain $|n_\Phi| \approx 10^{-2}$ at most.

Here, we plot the localization length of the critical state for metallic, zigzag nanotubes with different diameters. We define the localization length L by $|\phi_A^J|^2/|\phi_A^0|^2 \approx \exp(-3a_{cc}J/2L)$, where $3a_{cc}/2$ is the distance between the J and $J+1$ lines (Fig. 1). We obtain for $n_\Phi > \bar{n}_\Phi$,

$$\frac{L}{|C_h|}=\frac{1}{4\pi n_\Phi-\dfrac{\pi^2}{2\sqrt{3}n}}=\frac{1}{\dfrac{4\pi B}{B_n}-\dfrac{\pi^2}{2\sqrt{3}n}}. \qquad (11)$$

In Fig. 3, we plot $L/|C_h|$ for $n=30$, taken as the largest diameter for a SWCNT, and $n=51$, taken as a shell in a multiwalled carbon nanotube (MWCNT). The curvature-induced energy gaps are $E_{gap}=7.4$ meV and 2.6 meV, respectively, where we use $V_\pi=2.7$ eV. $\bar{n}_\Phi$ is estimated as 7.1 T for $n=30$ and 1.4 T for $n=51$. If we neglect the interlayer interaction in a MWCNT, a zigzag SWCNT in a MWCNT is the most suitable to examine the behavior of the critical states, because one does not need a strong magnetic field to close the curvature-induced minigap.

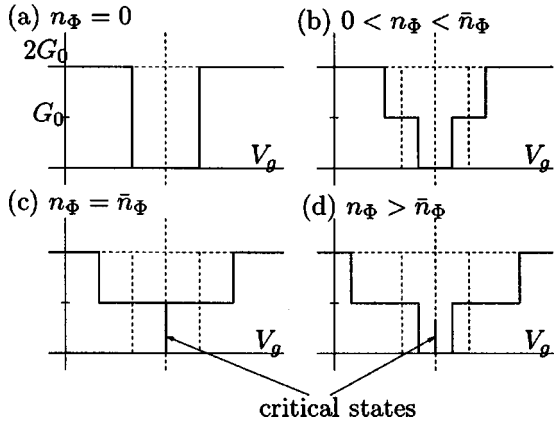

FIG. 4. Theoretical result of conductance with a metallic zigzag nanotube. We plot conductance as a function of gate voltage, V_g for several values of the AB flux.

The curvature effect and the modulation of the localization length can be experimentally proven by conductance measurements as a function of the gate voltage for various values of the AB flux. We plot the conductance for different n_Φ in Fig. 4, where we assume ideal contacts and zero temperature. Such measurement is attainable, as conductance of well-contacted individual SWCNTs was measured in the ballistic regime by Kong *et al.*[11] In Fig. 4(a), the solid curve represents conductance in the absence of the AB flux, $n_\Phi=0$. The zero-conductance state corresponds to the curvature-induced minigap. In Fig. 4(b), conductance changes according to the AB flux. Near the Fermi level, only one channel ($g \approx -1$) contributes to the transport and gives a unit of quantum conductance G_0. In Fig. 4(c), when $n_\Phi=\bar{n}_\Phi$, the zero-conductance state disappears and the critical states start to localize. Even when further AB flux is applied, there remains a finite conductance at the Fermi level due to the critical states, as is depicted in Fig. 4(d). However, because further AB flux quickly reduces the transmission probability from Fig. 3, the conductance at the Fermi level decreases.

The transition between the extended and localized states by the AB flux can be also understood in terms of the effective-mass theory of graphene. The effective-mass theory of low-energy dynamics is given by two Weyl equations,[12] each of which represents the dynamics around the K point and K' point in the momentum space. The curvature in the nanotube induces an effective gauge field in the Weyl equations,[9] and this gauge field gives the minigap of $2(\delta V_2-\delta V_1)$ through the AB effect. When we apply the AB flux ($n_\Phi<\bar{n}_\Phi$), the energy gap of one mode opens, while that of the other closes; therefore, the energy gap closes as a total system. If further magnetic flux ($n_\Phi>\bar{n}_\Phi$) is applied, some of the extended states become localized at the edges and their energy becomes zero, while other extended states open the gap again. Such zero-energy states cannot be obtained by solving the Weyl equations with a uniform energy gap in periodic systems. Instead, it is known that by locally modulating the energy gap, there appear localized states called

Jackiw-Rebbi (JR) states.[13] The edge states in the nanotube induced by the AB flux resemble the JR states, in that they have zero energy and are localized; meanwhile, they are different from ours because these edge states are induced by a uniform AB flux and not by a local modulation. We note that related states can appear when we introduce a local geometrical deformation in the nanotube.[10]

Throughout this paper, we have examined zigzag nanotubes having two Fujita's edges. Even for zigzag nanotubes with open edges, one can consider other cases with one or two edges being the Klein's edge.[14] If one of the edges is the Klein's edge and the other is the Fujita's edge, there are still localized states, whereas their properties are distinct from the previous case for the two Fujita's edges. Such a nanotube can be made by attaching A sites at the right edge of the zigzag nanotube in Fig. 1. The boundary condition for the right edge is $\epsilon\phi_A^{N+1}=\phi_B^N$. For the localized states we obtain $\epsilon=0$ and $\phi_A^J=(-g)^J\phi_A^0$, $\phi_B^J=0$ $(J=0,\ldots,N)$. Thus, the localized states have exactly $\epsilon=0$ for every value of g, and they have amplitude only on the A sublattice. Such states are localized near the right (left) edge when $|g|>1$ ($|g|<1$). Furthermore, there are no transitions between the localized and extended states, even when we apply a magnetic field. Meanwhile, when g passes $g=\pm 1$, the localized state with $\epsilon=0$ comes on the critical boundary of $\kappa^2=4$ in Fig. 2(a), and the corresponding localized state will move from the right edge to the left or vice versa and can be detected experimentally. On the other hand, when both edges are Klein's edges, the situation is somewhat similar to the case with two Fujita's edges. For this case, the localized states are realized when $|g|>1$ instead of $|g|<1$, and the AB flux induces a transition from the localized to the extended states.

Similar phenomena are expected also in nanotubes with other chiral structures, except for armchair nanotubes. Nakada *et al.* showed numerically that localized states appear not only in the zigzag edges, but also in edges with other shapes.[6] We expect that such localized states will undergo a transition with extended states in the presence of the AB flux.

Finally let us mention the Coulomb charging energy for the localized states. A typical energy scale of the charging energy for an edge state is $E_c\approx e^2/L_{\mathrm{edge}}$, where L_{edge} is the typical length for the edge states. This energy should be compared with that of the extended states evaluated as $E_c\approx e^2/L_{\mathrm{sys}}$, where L_{sys} is the system size. Since $L_{\mathrm{sys}}\gg L_{\mathrm{edge}}$, the Coulomb energy E_c for the edge states is much bigger than that of the extended states, and it may hinder localization. To lower this Coulomb charging energy, the spins of the localized states at each edge will align ferromagnetically.[4]

In addition to the edge states, the bulk states can also have interesting phenomena due to the AB flux in the SWCNTs. Namely, the AB flux induces a persistent current around the tube axis and gives an orbital magnetic moment.[15] The persistent current is caused by a splitting of the van Hove singularities by the AB flux.[16] Quite recently, the splitting was observed in semiconducting nanotubes as the splitting of the first subband magnetoabsorption peak[7] and also in small-band-gap (not curvature related) nanotubes as a temperature dependence of conductance.[8] These experiments were intended to observe that the AB flux can make an asymmetry between two energy bands composed of the extended (bulk) wave functions near the Fermi level. By means of doping in addition to the AB flux, an interference between many energy bands[17] takes place. This interference affects the magnetic and transport properties of the system, and it is helpful to get insight into the bulk electronic states.

In summary, the Aharonov-Bohm effect of carbon nanotubes is suited to examining not only the bulk electrical properties, but also the properties, of the edge states. We point out that there are two critical states in metallic, zigzag nanotubes. Although the critical states become extended due to the curvature effect in the absence of magnetic field, the Aharonov-Bohm flux can make a transition from the extended states into the localized edge states. This transition can be seen as a characteristic feature of conductance.

K. S. acknowledges support from the 21st Century COE Program of the International Center of Research and Education for Materials of Tohoku University. S. M. is supported by Grant-in-Aid (Grant No. 16740167) from the Ministry of Education, Culture, Sports, Science, and Technology (MEXT), Japan. R. S. acknowledges a Grant-in-Aid (Grant Nos. 13440091 and 16076201) from MEXT.

*Email address: sasaken@imr.edu

[1] R. Saito, G. Dresselhaus, and M. S. Dresselhaus, *Physical Properties of Carbon Nanotubes* (Imperial College Press, London, 1998).

[2] R. Saito, M. Fujita, G. Dresselhaus, and M. S. Dresselhaus, Phys. Rev. B **46**, 1804 (1992); N. Hamada, S. Sawada, and A. Oshiyama, Phys. Rev. Lett. **68**, 1579 (1992).

[3] M. Ouyang, J. Huang, C. L. Cheung, and C. M. Lieber, Science **292**, 27 (2001).

[4] M. Fujita, K. Wakabayashi, K. Nakada, and K. Kusakabe, J. Phys. Soc. Jpn. **65**, 1920 (1996).

[5] S. Okada and A. Oshiyama, J. Phys. Soc. Jpn. **72**, 1510 (2003).

[6] K. Nakada, M. Fujita, G. Dresselhaus, and M. S. Dresselhaus, Phys. Rev. B **54**, 17 954 (1996); M. Fujita, M. Igami, and K. Nakada, J. Phys. Soc. Jpn. **66**, 1864 (1997); K. Nakada, M. Igami, and M. Fujita, *ibid.* **67**, 2388 (1998); K. Wakabayashi, M. Fujita, H. Ajiki, and M. Sigrist, Phys. Rev. B **59**, 8271 (1999).

[7] S. Zaric, G. N. Ostojic, J. Kono, J. Shaver, V. C. Moore, M. S. Strano, R. H. Hauge, R. E. Smalley, and X. Wei, Science **304**, 1129 (2004).

[8] E. D. Minot, Y. Yaish, V. Sazonova, and P. L. McEuen, Nature (London) **428**, 536 (2004).

[9] C. L. Kane and E. J. Mele, Phys. Rev. Lett. **78**, 1932 (1997).

[10] K. Sasaki, Y. Kawazoe, and R. Saito, Prog. Theor. Phys. **113**, 4632005).

[11] J. Kong, E. Yenilmez, T. W. Tombler, W. Kim, H. Dai, R. B. Laughlin, L. Liu, C. S. Jayanthi, and S. Y. Wu, Phys. Rev. Lett.

87, 106801 (2001).
[12] J. C. Slonczewski and P. R. Weiss, Phys. Rev. **109**, 272 (1958); G. W. Semenoff, Phys. Rev. Lett. **53**, 2449 (1984).
[13] R. Jackiw and C. Rebbi, Phys. Rev. D **13**, 3398 (1976); see also, R. Jackiw, Dirac Prize Lecture, Trieste (1999), hep-th/9903255 (unpublished); G. 't Hooft and F. Bruckmann, hep-th/0010225 (unpublished); R. Rajaraman, cond-mat/0103366 (unpublished).
[14] D. J. Klein, Chem. Phys. Lett. **217**, 261 (1994).
[15] Y. Imry, *Introduction to Mesoscopic Physics*, 2nd ed. (Oxford University Press, Oxford, 2002).
[16] H. Ajiki and T. Ando, J. Phys. Soc. Jpn. **62**, 2470 (1993); Solid State Commun. **102**, 135 (1997).
[17] K. Sasaki, S. Murakami, and R. Saito, Phys. Rev. B **70**, 233406 (2004); S. Murakami, K. Sasaki, and R. Saito, J. Phys. Soc. Jpn. **73**, 3231 (2004).